Correlation effects in Sr_2RuO_4 and Ca_2RuO_4: Valence-band photoemission spectra and self-energy calculations

T. T. Tran,[1] T. Mizokawa,[1,2] S. Nakatsuji,[3] H. Fukazawa,[3] and Y. Maeno[3,4]
[1]*Department of Physics and Department of Complexity Science and Engineering, University of Tokyo, Chiba 277-8581, Japan*
[2]*PRESTO, Japan Science and Technology Agency, 4-1-8 Honcho Kawaguchi, Saitama, Japan*
[3]*Department of Physics, Kyoto University, Kyoto 606-8502, Japan*
[4]*International Innovation Center (IIC), Division of Research Initiatives, Kyoto University, Kyoto 606-8502, Japan*
(Received 20 May 2004; published 29 October 2004)

We have studied the electronic structure of Sr_2RuO_4 and Ca_2RuO_4 using x-ray photoemission spectroscopy (XPS) and subsequent model calculations. While the t_{2g} band of Sr_2RuO_4 has substantial spectral weight at the Fermi level, that of Ca_2RuO_4 has no spectral weight at E_F and shows a peak at -1.8 eV. In the valence-band XPS spectrum of Sr_2RuO_4, a satellite structure of the t_{2g} band is observed. In order to explain the spectral features, we have carried out band-structure calculations using the unrestricted Hartree-Fock (HF) approximation and found good agreement with the experimental result for Ca_2RuO_4. In order to explain the satellite structure of Sr_2RuO_4, we have performed second-order perturbation calculations of the self-energy corrections around the unrestricted HF solution of Sr_2RuO_4.

DOI: 10.1103/PhysRevB.70.153106 PACS number(s): 71.30.+h, 71.28.+d, 79.60.−i

Transition-metal oxides have been attracting considerable interest due to their rich physical properties such as metal-insulator transition, exotic superconductivity, and spin-charge-orbital ordering.[1,2] Among them is the newly discovered Mott transition system $Ca_{2-x}Sr_xRuO_4$, which shows a rich phase diagram including superconductor, paramagnetic metal, antiferromagnetic insulator, and paramagnetic insulator phases.[3] In order to understand the origin of this rich and complicated phase diagram, it is highly important to study the electronic structure of $Ca_{2-x}Sr_xRuO_4$ using spectroscopic methods. Although photoemission spectroscopy is a powerful technique to study the electronic structure of solids, one should pay attention to the surface sensitivity of photoemission spectroscopy in order to interpret the spectrum properly. In particular, the electronic structure of complicated transition-metal oxides may be considerably affected by the surface effect. The first ultraviolet photoemission studies of Sr_2RuO_4 (Refs. 4,5) have reported Fermi surfaces that were apparently different from the prediction of the band-structure calculations[6,7] and have raised serious controversy. Recently, Damascelli *et al.* have shown that the Sr_2RuO_4 surface prepared in suitable conditions gives the Fermi surface consistent with the band-structure calculation.[8] In addition, the theoretical study by Liebsch[9] has shown that the correlation effect is enhanced at the surface layer and that, in strongly correlated systems, the electronic structure of the surface can be very different from that of the bulk even without the surface reconstruction. Therefore, it is very important to study the electronic structure of the Ru oxides using x-ray photoemission spectroscopy that is more bulk sensitive than ultraviolet photoemission spectroscopy.

In the present work, we have examined the electronic structure of the end members Sr_2RuO_4 and Ca_2RuO_4 using x-ray photoemission spectroscopy (XPS) measurements that are rather bulk sensitive. Subsequently, we have analyzed the obtained valence-band photoemission spectra using model Hartree-Fock (HF) calculations and self-energy calculations. The comparison between the theoretical and experimental results indicates that the correlation effect beyond the Hartree-Fock treatment is much stronger in metallic Sr_2RuO_4 than in insulating Ca_2RuO_4.

Our XPS measurements were carried out at room temperature using a JPS9200 spectrometer. Monochromatic Al $K\alpha$ (1486.6 eV) radiation was used as an x-ray source. The pass energy of the electron analyzer was set to 10 eV. The total energy resolution including the x-ray source and the electron analyzer was about 0.6 eV. The binding energy was calibrated using the Fermi edge and the Au $4f$ core level (84.0 eV) of the gold reference sample. Single crystals of Sr_2RuO_4 and Ca_2RuO_4 grown using a floating zone method were cleaved *in situ*. The base pressure of the chamber was 7×10^{-8} Pa. The photoemission data were corrected at room temperature within 24 h after the cleavage. The angle θ between the surface normal and the outgoing photoelectron was set to be 20°.

The valence-band XPS spectra of Sr_2RuO_4 and Ca_2RuO_4 are shown in Fig. 1 (solid curves). At the photon energy of 1486.6 eV, the cross section of the Ru $4d$ subshell is dominant compared with that of O $2p$. Therefore, it is expected that the experimental results show up the Ru $4d$ spectra. The Ru $4d$ t_{2g} band of Sr_2RuO_4 has substantial spectral weight at the Fermi level (E_F), which is consistent with the metallic behavior of Sr_2RuO_4. In addition, the t_{2g} band shows a weak satellite structure at -1.5 eV, which is consistent with the previous photoemission study and theoretical calculations.[9] The intensity of the satellite structure is rather weak in the XPS spectrum compared to that in the ultraviolet photoemission spectrum of Sr_2RuO_4.[5] This is probably because the satellite formation is promoted by the enhanced correlation effect at the surface layer as pointed out by Liebsch.[9]

We have investigated the electronic structure of the layered perovskite Ca_2RuO_4 and Sr_2RuO_4 by using the multiband d-p model where full degeneracy of the Ru $4d$ and the O $2p$ are taken into account.[10] The model Hamiltonian is given by

 ©2004 The American Physical Society

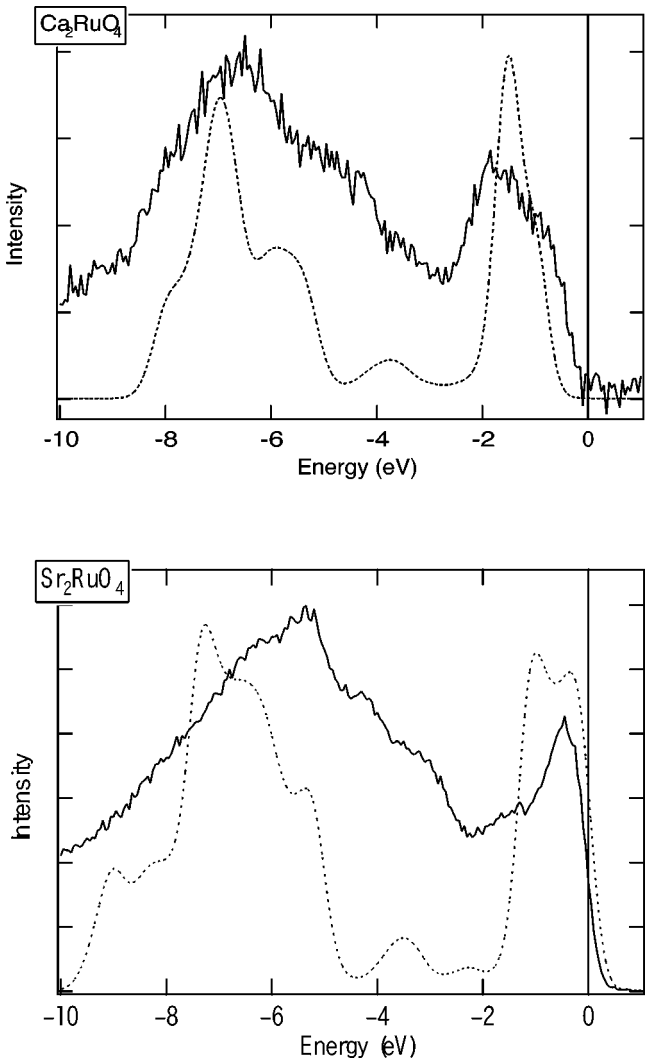

FIG. 1. Upper panel: Experimental result (solid curves) and calculated result by the model HF method (dotted curve) for Ca_2RuO_4. Lower panel: Those for Sr_2RuO_4.

$$H = H_p + H_d + H_{pd}, \tag{1}$$

$$H_p = \sum_{\mathbf{k},l,\sigma} \epsilon^p_{\mathbf{k}} p^\dagger_{\mathbf{k},l\sigma} p_{\mathbf{k},l\sigma} + \sum_{\mathbf{k},l>l',\sigma} V^{pp}_{\mathbf{k},ll'} p^\dagger_{\mathbf{k},l\sigma} p_{\mathbf{k},l'\sigma} + \text{H . c . }, \tag{2}$$

$$\begin{aligned} H_d = {} & \epsilon^0_d \sum_{i,m,\sigma} d^\dagger_{i,m\sigma} d_{i,m\sigma} + \sum_{m,m',\sigma,\sigma'} h_{m,\sigma,m',\sigma'} d^\dagger_{i,m\sigma} d_{i,m'\sigma'} \\ & + u \sum_{i,m} d^\dagger_{i,m\uparrow} d_{i,m\uparrow} d^\dagger_{i,m\downarrow} d_{i,m\downarrow} + u' \sum_{i,m\neq m'} d^\dagger_{i,m\uparrow} d_{i,m\uparrow} d^\dagger_{i,m'\downarrow} d_{i,m'\downarrow} \\ & + (u' - j') \sum_{i,m>m',\sigma} d^\dagger_{i,m\sigma} d_{i,m\sigma} d^\dagger_{i,m'\sigma} d_{i,m'\sigma} \\ & + j' \sum_{i,m\neq m'} d^\dagger_{i,m\uparrow} d_{i,m'\uparrow} d^\dagger_{i,m\downarrow} d_{i,m'\downarrow} \\ & + j \sum_{i,m\neq m'} d^\dagger_{i,m\uparrow} d_{i,m'\uparrow} d^\dagger_{i,m'\downarrow} d_{i,m\downarrow}, \end{aligned} \tag{3}$$

TABLE I. Parameter sets for Ca_2RuO_4 and Sr_2RuO_4.

	$(pd\sigma)$ (eV)	r (deg)	t (deg)	δ_{JT}
Ca_2RuO_4	−2.8	12.5	10	0.975
Sr_2RuO_4	−3.4	0	0	1.025

$$H_{pd} = \sum_{\mathbf{k},l,m,\sigma} V^{pd}_{\mathbf{k},lm} d^\dagger_{\mathbf{k},m\sigma} p_{\mathbf{k},l\sigma} + \text{H . c.} \tag{4}$$

$d^\dagger_{i,m\sigma}$ are creation operators for the 4d electrons at site i. $d^\dagger_{\mathbf{k},m\sigma}$ and $p^\dagger_{\mathbf{k},l\sigma}$ are creation operators for Bloch electrons with wave vector $\mathbf{k}$ constructed from the Ru 4d and O 2p orbitals, respectively. $h_{m,\sigma,m',\sigma'}$ represents the crystal field and spin-orbit interaction of the 4d orbital. The magnitude of the spin-orbit interaction is 0.15 eV for the Ru 4d orbital. The intra-atomic Coulomb interactions between 4d electrons are given by Kanamori parameters, u, u', j, and j'. The transfer integrals between the Ru 4d and O 2p orbitals $V^{pd}_{\mathbf{k},lm}$ are given in terms of Slater-Koster parameters $(pd\pi)$ and $(pd\sigma)$. The transfer integrals between 2p orbitals $V^{pp}_{\mathbf{k},ll'}$ are expressed by $(pp\sigma)$ and $(pp\pi)$. Here, the ratio $(pd\sigma)/(pd\pi)$ is −2.2. The present model takes into account the spin-orbit interaction and the lattice distortion such as Jahn-Teller distortion, tilting, and rotation of RuO_6 octahedron. In the present calculation, u, u' are, respectively, 2.5 eV, 1.5 eV; $j=j'=0.5$ eV. $(pp\sigma)$ and $(pp\pi)$ are fixed at 0.60 and −0.15 eV, respectively, for the undistorted lattice. The transfer integrals between Ru 4d and O 2p orbitals are adjusted to get a good agreement with the LDA results; the values of rotation angle r, the tilting angle t, and the Jahn-Teller distortion δ_{JT} are from the previous work of Friedt *et al.*[11] These values are listed in Table I. When the lattice is distorted, the transfer integrals are scaled using Harrison's law.

The HF mean-field treatment is applied to the two-body Hamiltonian terms in H_d by replacing, for example, $u\Sigma_{i,m} d^\dagger_{i,m\uparrow} d_{i,m\uparrow} d^\dagger_{i,m\downarrow} d_{i,m\downarrow}$ by its average value:[12]

$$\begin{aligned} u \sum_{i,m} d^\dagger_{i,m\uparrow} d_{i,m\uparrow} d^\dagger_{i,m\downarrow} d_{i,m\downarrow} = {} & u \sum_{i,m} \langle d^\dagger_{i,m\uparrow} d_{i,m\uparrow} \rangle d^\dagger_{i,m\downarrow} d_{i,m\downarrow} \\ & + u \sum_{i,m} d^\dagger_{i,m\uparrow} d_{i,m\uparrow} \langle d^\dagger_{i,m\downarrow} d_{i,m\downarrow} \rangle \\ & - u \sum_{i,m} \langle d^\dagger_{i,m\uparrow} d_{i,m\uparrow} \rangle \langle d^\dagger_{i,m\downarrow} d_{i,m\downarrow} \rangle. \end{aligned}$$

In the Hartree-Fock calculation, we input initial values of the order parameters such as $\langle d^\dagger_{i,m\uparrow} d_{i,m\uparrow} \rangle$ and diagonalized the mean-field Hamiltonian to get a set of eigenfunctions. The new values of the order parameters were then calculated at these eigenfunctions. These self-consistency cycles were iterated until successive differences of all the order parameters converged to less than 2×10^{-4} by sampling 40 000 k points in the first Brillouin zone. The single-electron excitation spectrum was then calculated from the HF results by using Koopmans's theorem.

Our calculated spectra of Ca_2RuO_4 and Sr_2RuO_4 within the HF approximation are shown in Fig. 1 together with the

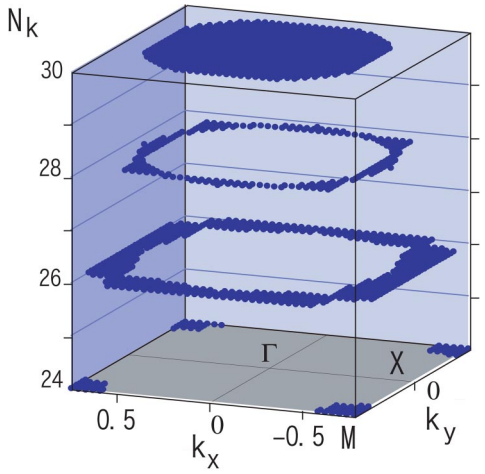

FIG. 2. $N_{\mathbf{k}}$ plot of Sr_2RuO_4.

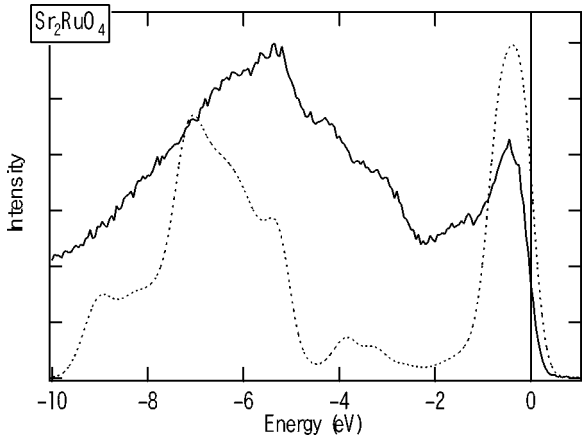

FIG. 3. Experimetal (dotted) and calculated (solid) results for Sr_2RuO_4.

experimental results. The calculated results are further broadened considering the energy resolution of the experimental setup. We observed a good agreement between calculated and experimental results in positions and intensities of the main peaks for Ca_2RuO_4. From our calculation, we can conclude that the two main peaks at around −1.8 eV and −6.2 eV are of the partial Ru 4*d* contribution from, respectively, the Ru $4d_{t_{2g}}$–O 2*p* antibonding band and the Ru $4d_{t_{2g}}$–O 2*p* bonding band. The asymmetric line shape of the Ru $4d_{t_{2g}}$–O 2*p* antibonding band (Ru t_{2g} band) is also reproduced by the calculation. For Sr_2RuO_4, our HF calculation gives a similar result of the Fermi surface to that obtained from the local density approximation (LDA) calculation by Oguchi[6] with two electronlike surfaces around Γ and one holelike surface around *M* (see Fig. 2). However, comparing with the experimental result (Fig. 1), the calculated Ru t_{2g} band near the Fermi level is too broad, and the relative intensities of the two peaks near the Fermi level do not match the experimental result.

The calculated Fermi surface of Sr_2RuO_4 is presented by mapping N_k, which is the number of occupied state at each momentum *k*:

$$N_{\mathbf{k}} = \sum_{m,\sigma} \langle d^{\dagger}_{\mathbf{k},m\sigma} d_{\mathbf{k},m\sigma} \rangle + \sum_{l,\sigma} \langle p^{\dagger}_{\mathbf{k},l\sigma} p_{\mathbf{k},l\sigma} \rangle .$$

The $N_{\mathbf{k}}$ plot as a function of k_x and k_y is shown in Fig. 2. As mentioned above, the calculated result agrees with the prediction of LDA calculation[6,7] as well as the observation of angle-resolved photoemission spectroscopy.[8]

In an attempt to explain the band narrowing and the satellite structure observed in the Ru t_{2g} band, we have tried to take the electron-correlation effect into our calculation through perturbation calculations. The Dyson equation for the full Green's function is

$$[\tilde{\omega} - \mathbf{H}^{HF} - \Sigma_{\mathbf{k},\sigma}(\tilde{\omega})]\mathbf{G}_{\mathbf{k},\sigma}(\tilde{\omega}) = 1, \tag{5}$$

where $\tilde{\omega} = \omega - \mu + i\delta$, ω denotes the energy dependence, μ is the chemical potential, and δ is a positive infinitesimal. In our calculation, $\mathbf{G}_{\mathbf{k},\sigma}(\tilde{\omega})$ is a 34×34 matrix and the basis set for $\mathbf{G}_{\mathbf{k},\sigma}(\tilde{\omega})$ is Ru 4*d* and O 2*p*. $\Sigma^{pp} = 0$ while $\Sigma^{dd}_{\mathbf{k},\sigma}(\tilde{\omega})$ is constructed to second order in u, u', j, and j' using the eigenenergy $\varepsilon^{n}_{\sigma}(\mathbf{k})$ and the weight of the *m*th 4*d* orbital $\alpha^{n,m}_{\sigma}(\mathbf{k})$ in the Bloch orbitals yielded from HF calculation:

$$\Sigma^{dd}_{\mathbf{k},\sigma}(\tilde{\omega}) = \Sigma^{(1)dd}_{\sigma} + \Sigma^{(2)dd}_{\mathbf{k},\sigma}(\tilde{\omega}). \tag{6}$$

Here, *n* is the band index and **k** is the wave vector. The form of $\Sigma^{dd}_{\mathbf{k},\sigma}(\tilde{\omega})$ is similar to that used in the paper of Steiner *et al.*[13] For metallic Sr_2RuO_4, the self-energy must satisfy $\mathrm{Im}[\Sigma_{\mathbf{k},\sigma}(\omega)] = 0$ at the Fermi level,[14,15] this can be overcome by calculating $\Sigma_{\mathbf{k},\sigma}(\omega)$ self-consistently.

The spectral function $\mathbf{A}_{\mathbf{k},\sigma}(\tilde{\omega})$ is calculated once we get $\mathbf{G}_{\mathbf{k},\sigma}(\tilde{\omega})$ from Eq. (5):

$$\mathbf{A}_{\mathbf{k},\sigma}(\tilde{\omega}) = -\frac{1}{\pi}\mathrm{Im}[\mathbf{G}_{\mathbf{k},\sigma}(\tilde{\omega})]. \tag{7}$$

Summing $\mathbf{A}_{\mathbf{k},\sigma}(\tilde{\omega})$ over **k** gives us the spectral function that should be compared with the valence-band XPS spectrum.

The calculation result for Sr_2RuO_4 with the self-energy correction is shown in Fig. 3. The inclusion of the self-energy correction reduced the bandwidth of the t_{2g} band near the Fermi level, which shows an improvement comparing with the HF result. The tail of the t_{2g} band is obtained, which can be attributed to the weak satellite structure observed in the photoemission spectrum. However, the intensity of the satellite structure is not well reproduced in the present calculation. Also, the calculated result cannot reproduce the line shape of the bonding Ru-O band located around −6 eV. Probably, we need to consider the higher-order terms in the self-energy.[9]

In conclusion, we have performed the XPS measurement of Ca_2RuO_4 and Sr_2RuO_4 and observed a satellite structure in the t_{2g} band of Sr_2RuO_4. Also, we have performed model calculations to explain the XPS spectra in the valence band. The model HF calculation results show good agreement with the experimental result for Ca_2RuO_4 but do not reproduce the spectrum of Sr_2RuO_4 well. This implies that the electron correlation in metallic Sr_2RuO_4 is stronger and is more com-

plicated than in insulating Ca_2RuO_4 and cannot be treated within the HF theory. We take into account the electron correlations in Sr_2RuO_4 by performing the self-energy corrections around the HF solution of Sr_2RuO_4. The result showed a better agreement with valence-band XPS spectrum compared to the HF result.

This work was supported by the Ministry of Education, Culture, Sports, Science and Technology of Japan.

[1] Y. Tokura and N. Nagaosa, Science **288**, 462 (2000).
[2] M. Imada, A. Fujimori, and Y. Tokura, Rev. Mod. Phys. **70**, 1039 (1988).
[3] S. Nakatsuji and Y. Maeno, Phys. Rev. Lett. **84**, 2666 (2000).
[4] T. Yokoya, A. Chainani, T. Takahashi, H. Katayama-Yoshida, M. Kasai, and Y. Tokura, Phys. Rev. Lett. **76**, 3009 (1996).
[5] D. H. Lu, M. Schmidt, T. R. Cummins, S. Schuppler, F. Lichtenberg and J. G. Bednorz, Phys. Rev. Lett. **76**, 4845 (1996).
[6] T. Oguchi, Phys. Rev. B **51**, 1385 (1995).
[7] D. J. Singh, Phys. Rev. B **52**, 1358 (1995).
[8] A. Damascelli, D. H. Lu, K. M. Shen, N. P. Armitage, F. Ronning, D. L. Feng, C. Kim, Z.-X. Shen, T. Kimura, Y. Tokura, Z. Q. Mao, and Y. Maeno, Phys. Rev. Lett. **85**, 5194 (2000).
[9] A. Liebsch, Phys. Rev. Lett. **90**, 096401 (2003).
[10] M. Kurokawa and T. Mizokawa, Phys. Rev. B **66**, 024434 (2002).
[11] O. Friedt, M. Braden, G. Andre, P. Adelman, S. Nakatsuji, and Y. Maeno, cond-mat/0007218 (unpublished).
[12] T. Mizokawa and A. Fujimori, Phys. Rev. B **54**, 5368 (1996).
[13] M. M. Steiner, R. C. Albers, and L. J. Sham, Phys. Rev. B **45**, 13272 (1992).
[14] T. Mizokawa and A. Fujimori, Phys. Rev. B **53**, R4201 (1996).
[15] C. Calandra and F. Manghi, Phys. Rev. B **45**, 5819 (1992).